Search for Milli-Charged particles from the Sun at IceCube

Ye Xu

School of Electronic, Electrical Engineering and Physics, Fujian University of Technology,
Fuzhou 350118, China

Research center for Microelectronics Technology, Fujian University of Technology,
Fuzhou 350118, China

E-mail: xuy@fjut.edu.cn

ABSTRACT: It is assumed that heavy dark matter particles ϕ with O(TeV) mass captured by the Sun may decay to relativistic light milli-charged particles (MCPs). These MCPs could be measured by the IceCube detector. The massless hidden photon model was taken for MCPs to interact with nuclei, so that the numbers and fluxes of expected MCPs and neutrinos may be evaluated at IceCube. Based on the assumption that no events are observed at IceCube in 6 years, the corresponding upper limits on MCP fluxes were calculated at 90% C. L. These results indicated that MCPs could be directly detected in the secondaries' energy range O(100GeV)-O(10TeV) at IceCube, when $\epsilon^2 \gtrsim 10^{-10}$. And a new region of $0.6\,\mathrm{MeV} < m_{MCP} < 10\,\mathrm{MeV}$ and $6 \times 10^{-6} < \epsilon \lesssim 10^{-4}$ is ruled out in the m_{MCP}-ϵ plane with 6 years of IceCube data.

Contents

1 Introduction

It was found in cosmological and astrophysical observations that most (84%) of matter in the Universe consists of dark matter (DM) [1–3]. So far, DM has been observed only through its gravitational interactions. DM is neutral under all Standard Model (SM) gauge interactions in most of DM models, for example, weak interacting massive particles (WIMPs), axions, axion-like particles, sterile neutrinos and so on. Unfortunately, no one has found those neutral DM particles yet [4–14].

Milli-charged particles (MCPs), which are fermions, with a small electric charge ϵe (e is the electric charge for an electron and $\epsilon \ll 1$), are an alternative DM scenario [15–17]. A model with a hidden gauge group U(1) is taken for MCPs to interact with nuclei. A second unbroken "mirror" U(1)$'$ was introduced in this model. The corresponding massless hidden photon field may have a kinetic mixing to the SM photon, so that a MCP under U(1)$'$ appears to have a small coupling to the SM photon [18]. Certainly, MCPs can also arise in extra-dimensional scenarios or as hidden magnetic monopoles receiving their mass from a magnetic mixing effect [19–21]. ϵ is also the kinetic mixing parameter between those two kinds of photons. The searches for MCPs have been performed in cosmological and astrophysical observations, accelerator experiments, experiments for decay of ortho-positronium and Lamb shift, DM searches and so on, so that constraints on ϵ were determined by those observations. [15, 22–29].

In the DM scenario in this work, there exist at least two DM species in the Universe (for example, O(TeV) DM and light MCPs). O(TeV) DM, ϕ, is a thermal particle which is generated by the early universe. The bulk of present-day DM consists of them. The other is a stable light fermion, MCP (χ), which is the product of the decay of ϕ ($\phi \to \chi\bar{\chi}$), like the DM decay channel mentioned in ref. [30]. It is assumed that its mass is much less than that of a proton. Due to the decay of long-living ϕ ($\tau_\phi \gg t_0$ [31, 32], $t_0 \sim 10^{17}$ s is the age of the Universe. Here $\tau_\phi \geq 10^{19}$ s), the present-day DM may also contain a very small

component which is MCPs with the energy of about $\frac{m_\phi}{2}$. Here it is assumed that the decay of ϕ are only through $\phi \to \chi\bar{\chi}$.

The ϕ's of the Galactic halo would be captured by the Sun when their wind sweeps through the Sun. The measurement of light neural DM due to the decay of heavy ϕ captured by the Sun at IceCube has been discussed in my previous work [33]. The Z'-portal model was taken for those neural particles to interact with nuclei. In this work, however, the ϕ's captured by the Sun can only decay into MCPs. A model with a massless hidden photon will be taken for MCPs to interact with nuclei. MCPs would interact with nuclei when they pass through the Sun, the Earth and ice. Those MCPs can be directly measured with the IceCube neutrino telescope via the deep inelastic scattering (DIS) with nuclei in the ice. The capability of the measurement of those particles will also be discussed here. In this measurement, the background consists of muons and neutrinos generated in cosmic ray interactions in the Earth's atmosphere and astrophysical neutrinos.

2 Flux of MCPs which reach the Earth

The ϕ's of the Galactic halo would collide with atomic nuclei in the Sun and be captured when their wind sweeps through the Sun. Those ϕ's inside the Sun can decay into MCPs at an appreciable rate. Then the number of those ϕ's is obtained in the way in ref. [34]

$$\frac{dN}{dt} = C_{\text{cap}} - 2\Gamma_{\text{ann}} - C_{\text{evp}}N - C_{\text{dec}}N \tag{2.1}$$

where C_{cap}, Γ_{ann} and C_{evp} are the capture rate, the annihilation rate and the evaporation rate, respectively. The evaporation rate is only relevant when the DM mass $< 5\,\text{GeV}$ [34], which are much lower than my interested mass scale (the mass of ϕ, $\text{m}_\phi \geq 1\,\text{TeV}$). Thus their evaporation contributes to the accumulation in the Sun at a negligible level in the present work. C_{dec} is the decay rate for ϕ's. Since the fraction of ϕ decay $\leq 3.0 \times 10^{-12}$ per year ($\tau_\phi \geq 10^{19}$ s), its contribution to the ϕ accumulation in the Sun can be ignored in the evaluation of ϕ accumulation. Γ_{ann} is obtained by the following equation [34]

$$\Gamma_{\text{ann}} = \frac{C_{\text{cap}}}{2} tanh^2 \left(\frac{t}{\tau}\right) \approx \frac{C_{\text{cap}}}{2} \quad with \quad t \gg \tau \tag{2.2}$$

where $\tau = (C_{\text{cap}} C_{\text{ann}})^{-\frac{1}{2}}$ is a time-scale set by the competing processes of capture and annihilation. At late times $t \gg \tau$ one can approximate $tanh^2 \frac{t}{\tau} = 1$ in the case of the Sun [34]. C_{cap} is proportional to $\frac{\sigma_{\phi N}}{m_\phi}$ [34, 35], where m_ϕ is the mass of ϕ and $\sigma_{\phi N}$ is the scattering cross section between the nuclei and ϕ's. The spin-independent cross section is only considered in the capture rate calculation. Then $\sigma_{\phi N}$ is taken to be 10^{-44} cm^2 for $m_\phi \sim \text{O(TeV)}$ [4, 5]. Besides, one knows that ϕ's are concentrated around the center of the Sun from ref. [34].

The MCPs which reach the Earth are produced by the decay of ϕ's in the Sun's core. Those MCPs have to pass through the Sun and interact with nuclei inside the Sun. Then

the number N_s of MCPs which reach the Sun's surface is obtained by the following equation:

$$N_s = 2N_0 \left(exp\left(-\frac{t_0}{\tau_\phi}\right) - exp\left(-\frac{t_0+T}{\tau_\phi}\right) \right) \prod_{i=1}^{n=\mathcal{N}} exp\left(-\frac{\delta L}{L_i}\right) \qquad with \quad T \ll \tau_\phi$$
(2.3)
$$\approx 2N_0 \frac{T}{\tau_\phi} exp\left(-\frac{t_0}{\tau_\phi}\right) \prod_{i=1}^{n=\mathcal{N}} exp\left(-\frac{\delta L}{L_i}\right)$$

where $N_0 = \int_0^{t_s} \frac{dN}{dt} dt$ is the number of ϕ's captured in the Sun. t_s and t_0 are the ages of the Sun and the Universe, respectively. T is the lifetime of taking data for IceCube and taken to be 6 years. If the distance from the Sun's center to the Sun's surface is equally divided into $\mathcal{N}$ portions, $\delta L = \frac{R_{\rm sun}}{\mathcal{N}}$. $L_i = \frac{1}{N_A\rho_i\sigma_{\chi N}}$ is the MCP interaction length at i×δL away from the Sun's center. ρ_i is the density at i×δL away from the Sun's center [36]. N_s is computed in column density in the present work. The first exponential term in eq. (2.3) is the fraction of decay of ϕ's in the Sun's core. The term of continued product in eq. (2.3) is the faction of MCPs which reach the Sun's surface. Here $\mathcal{N}$ is taken to be 10^4. The results with $\mathcal{N}=10^4$ is sufficiently accurate, whose uncertainty is about 0.05%.

Then the flux Φ_{MCP} of MCPs, which reach the Earth, from the Sun's core is described by

$$\Phi_{MCP} = \frac{N_s}{4\pi D_{se}^2}$$
(2.4)

where D_{se} is the distance between the Sun and Earth.

3 MCP and neutrino interactions with nuclei

In this work, the hidden photon model [18] is taken for MCPs to interact with nuclei via a neural current (NC) interaction mediated by the mediator generated by the kinetic mixing between the SM and massless hidden photons. There is only a well-motivated interaction allowed by SM symmetries that provide a "portal" from the SM particles into the MCPs. This portal is $\frac{\epsilon}{2}F_{\mu\nu}F'^{\mu\nu}$. Then its interaction Lagrangian can be written as follows:

$$\mathcal{L} = \sum_q e_q \bar{q}\gamma^\mu q A_\mu - \frac{1}{4}F'_{\mu\nu}F'^{\mu\nu} + \bar{\chi}(i\slashed{D} - m_\chi)\chi - \frac{\epsilon}{2}F_{\mu\nu}F'^{\mu\nu}$$
(3.1)

where the sum runs over quark flavors in the nucleon and e_q is the electric charge of the quark. A_μ is the vector potential of the SM photon. $F'_{\mu\nu}$, $F_{\mu\nu}$ are the field strength tensor of the hidden and SM photons, respectively. m_χ is the MCP's mass. ϵ is the kinetic mixing parameter between the SM and hidden photons. The covariant derivative is

$$D_\mu = \partial_\mu - ig_\chi A'_\mu$$
(3.2)

where g_χ is the gauge coupling of the U(1)$'$ and A'_μ is the vector potential of the hidden photon.

Then we may calculate the cross sections for scattering of MCP on an isoscalar nucleon target N=(p+n)/2 at high energies. Those DIS cross sections mainly depends on the

behavior of structure functions at small x, which is the Bjorken scaling parameter. Since the MCP-mediator coupling is equal to $\epsilon^2\alpha$, the DIS cross section of MCPs on nuclei is equivalent to ϵ^2 times as much as that of electrons on nuclei via a NC interaction under electromagnetism, that is

$$\sigma_{\chi N} \approx \epsilon^2 \sigma_{eN}^{\gamma} \tag{3.3}$$

where χ denotes a MCP with ϵe, N is a nucleon. σ_{eN}^{γ} is the cross section depending on γ exchange between elections and nuclei. That electron-nuclei cross section can be obtained by integrating over the following doubly differential cross section may be expressed in term of the structure functions as

$$\frac{d^2\sigma_{eN}^{\gamma}}{dxdQ^2} = \frac{2\pi\alpha^2}{xQ^4}\left[Y_+\tilde{F}_2\left(x,Q^2\right) - y^2\tilde{F}_L\left(x,Q^2\right)\right] \tag{3.4}$$

where Q^2 is the momentum transfer, α is the fine-structure constant. $Y_+ = 1 + (1-y)^2$, the inelasticity parameter $y = \dfrac{Q^2}{2m_N E_{\text{in}}}$. $\tilde{F}_2(x,Q^2)$ and $\tilde{F}_L(x,Q^2)$ are the generalized structure functions which depend on γ exchange between the electrons and nuclei. m_N is the nucleon mass, E_{in} is the incident electron energy (also the incident MCP energy). According to Next-to-leading (NLO) order QCD calculations, since, the contribution of the longitudinal structure function $\tilde{F}_L(x,Q^2)$ to that cross section is less than 1% [37], $\tilde{F}_L(x,Q^2)$ is ignored in this work. The $\tilde{F}_2(x,Q^2)$ term under electromagnetism is equal to a term depending on γ exchange (F_2^{γ}), that is

$$\tilde{F}_2 = F_2^{\gamma} \tag{3.5}$$

The structure function F_2^{γ} can be expressed in terms of the quark and anti-quark parton distribution functions (PDFs) as

$$F_2^{\gamma} = \sum_q e_q^2 x(q + \bar{q}) \tag{3.6}$$

where the sum runs over quark flavors except the top quark (it is too massive to contribute significantly in the region of interest). A set of PDFs was determined with the LHC run II data [38]. This set of PDFs was taken to calculate the cross section for scattering of MCPs on nuclei in this work. For the PDFs of sea quarks, here, $s_s = \bar{s}_s = c_s = \bar{c}_s = b_s = \bar{b}_s$ was assumed in the calculation of those cross sections.

The total DIS cross sections of MCPs on nuclei may be obtained through integrating over eq. (3.4) and calculating eq. (3.3). Their results can be approximately expressed as a simple power-law form in the energy range 1 TeV-10 PeV

$$\sigma_{\chi N} \approx 1.756 \times 10^{-31}\epsilon^2 cm^2 \left(\frac{E_\chi}{1GeV}\right)^{0.179} \tag{3.7}$$

where E_χ is the MCP energy.

The DIS cross-section for neutrino interaction with nuclei is computed in the lab-frame and given by simple power-law forms [39] for neutrino energies above 1 TeV:

$$\sigma_{\nu N}(CC) = 4.74 \times 10^{-35} cm^2 \left(\frac{E_\nu}{1\,GeV} \right)^{0.251} \tag{3.8}$$

$$\sigma_{\nu N}(NC) = 1.80 \times 10^{-35} cm^2 \left(\frac{E_\nu}{1\,GeV} \right)^{0.256} \tag{3.9}$$

where $\sigma_{\nu N}(CC)$ and $\sigma_{\nu N}(NC)$ are the DIS cross sections for neutrino scattering on nuclei via the charge current (CC) and neutral current (NC) interactions, respectively. E_ν is the neutrino energy.

The inelasticity parameter $y = 1 - \frac{E_{\chi',lepton}}{E_{in}}$ (where E_{in} is the incident MCP or neutrino energy and $E_{\chi',lepton}$ is the outgoing MCPs or lepton energy). $E_{sec} = yE_{in}$, where E_{sec} is the secondaries' energy after a MCP or neutrino interaction with nuclei. The mean values of y for MCPs have been computed:

$$\langle y \rangle = \frac{1}{\sigma(E_{in})} \int_0^1 y \frac{d\sigma}{dy}(E_{in}, y)dy \tag{3.10}$$

The MCP and neutrino interaction lengths can be obtained by

$$L_{\nu,\chi} = \frac{1}{N_A \rho \sigma_{\nu,\chi N}} \tag{3.11}$$

where N_A is the Avogadro constant, and ρ is the density of matter, which MCPs and neutrinos interact with.

4 Evaluation of the numbers of expected MCPs and neutrinos at IceCube

The IceCube detector is deployed in the deep ice below the geographic South Pole [40]. It can detect neutrino interactions with nuclei via the measurement of the cascades caused by their secondary particles above the energy threshold of 100 GeV [41]. The MCPs which pass through the IceCube detector would interact with the nuclei inside IceCube. This is similar to the NC DIS of neutrino interaction with nuclei, whose secondary particles would develop into a cascade at IceCube.

MCP events were selected with the following event selection criteria in this analysis. First, only cascade events were kept. To reduce more background events initiated by atmospheric muon, Second, only up-going events occurring during a period in which the Sun was below the horizon were kept. Besides, only those up-going events from the Sun's direction were kept.

The C_1 and C_2 factors should be considered in the evaluation of the numbers of expected MCPs. C_1 is equal to 68.3% (that is 68.3% of the MCP events reconstructed with IceCube fall into a window caused by one standard energy uncertainty). C_2 is equal to 50% (that is 50% of the MCP events reconstructed with IceCube fall into a window caused

by one median angular uncertainty). Then the number N_{det} of expected MCPs obeys the following equation:

$$\frac{dN_{\text{det}}}{dE} = C_1 \times C_2 \times \int_T A_{\text{eff}}(E) \Phi_{MCP} P(E, \xi(t)) dt \tag{4.1}$$

where $A_{\text{eff}}(E)$ obtained from the figure 2 in ref. [41] is denoting the effective observational area for IceCube. E is denoting the energy of an incident particle. $P(E, \xi(t))$ can be given by the following equation:

$$P(E, \xi(t)) = exp\left(-\frac{D_e(\xi(t))}{L_{\text{earth}}}\right)\left(1 - exp(-\frac{D}{L_{\text{ice}}})\right). \tag{4.2}$$

where $L_{\text{earth,ice}}$ is denoting the MCP interaction lengths with the Earth and ice, respectively. D is denoting the effective length in the IceCube detector and taken to be 1 km in this work. $D_e(\xi(t)) = 2R_e sin(\xi(t))$ is denoting the distance through the Earth. R_e is denoting the radius of the Earth. $\xi(t)$ is denoting the obliquity of the ecliptic changing with time. The maximum value of ξ is 23.44°.

After rejecting track-like events, the background remains two sources: astrophysical and atmospheric neutrinos which pass through the detector of IceCube. Only a neural current interaction with nuclei is relevant to muon neutrinos considered here. The astrophysical neutrinos flux can be described by [42]

$$\Phi_\nu^{\text{astro}} = \Phi_{\text{astro}} \times \left(\frac{E_\nu}{100TeV}\right)^{-\left(\alpha + \beta log_{10}\left(\frac{E_\nu}{100TeV}\right)\right)} \times 10^{-18} GeV^{-1} cm^{-2} s^{-1} sr^{-1} \tag{4.3}$$

where Φ_ν^{astro} is denoting the total astrophysical neutrino flux. The coefficients, Φ_{astro}, α and β are given in figure VI.10 in ref. [42]. The atmospheric neutrinos flux can be described by [43]

$$\Phi_\nu^{\text{atm}} = C_\nu \left(\frac{E_\nu}{1GeV}\right)^{-\left(\gamma_0 + \gamma_1 x + \gamma_2 x^2\right)} GeV^{-1} cm^{-2} s^{-1} sr^{-1} \tag{4.4}$$

where $x = log_{10}(E_\nu/1GeV)$. Φ_ν^{atm} is denoting the atmospheric neutrino flux. The coefficients, C_ν (γ_0, γ_1 and γ_2) are given in table III in ref. [43].

The neutrinos fallen into the energy and angular windows mentioned above would also be regarded as signal candidate events, so the evaluation of the number of expected neutrinos has to be performed by integrating over the region caused by these windows. Then the number of expected neutrinos N_ν obeys the following equation:

$$\frac{dN_\nu}{dE} = \int_T \int_{\theta_{\min}}^{\theta_{\max}} A_{\text{eff}}(E) \left(\Phi_\nu^{\text{astro}} + \Phi_\nu^{\text{atm}}\right) P(E, \xi(t), \theta) \frac{2\pi r_e(\xi(t))^2 sin2\theta}{D'_e(\epsilon(t), \theta)^2} d\theta dt \tag{4.5}$$

where $r_e(\xi(t)) = \frac{D_e(\xi(t))}{2}$. θ is denoting the angular separation between the neutrinos and the Sun's diretion. $\theta_{\min} = 0$ and $\theta_{\max} = \sigma_\theta$. σ_θ is denoting the median angular uncertainty for cascades at IceCube. The standard energy and median angular uncertainties can be obtained from the ref. [44] and ref. [45], respectively. $P(E, \xi(t), \theta)$ can be given by

$$P(E, \xi(t), \theta) = exp\left(-\frac{D'_e(\xi(t), \theta)}{L_{\text{earth}}}\right)\left(1 - exp\left(-\frac{D}{L_{\text{ice}}}\right)\right) \tag{4.6}$$

where $D'_e(\xi(t), \theta) = D_e(\xi(t))cos(\theta)$ is denoting the distance through the Earth.

5 Results

The distributions and numbers of expected MCPs and neutrinos were evaluated in the secondaries' energy range 100 GeV-100 TeV assuming 6 years of IceCube data. Figure 1 shows the distributions with an energy bin of 100 GeV of expected MCPs and neutrinos. Compared to MCPs with $\epsilon^2 = 10^{-10}$ and $\tau_\phi = 10^{19}$ s, the numbers of neutrino events per energy bin are at least smaller by 4 orders of magnitude in the energy range 100 GeV-100 TeV. As shown in figure 1, the dominant background is caused by atmospheric neutrinos at energies below 5 TeV but astrophysical neutrinos at energies above about 10 TeV in this measurement.

The numbers of expected neutrinos (see black dash line) are shown in figure 2. The evaluation of the numbers of expected neutrinos was performed through integrating over the region caused by the energy and angular windows described above. The black dot line denotes the number of expected atmospheric neutrinos. This figure indicates the neutrino background can be ignored at the secondary energies above 300 GeV in this measurement. The numbers of expected MCPs with $\epsilon^2 = 10^{-8}$ and $\tau_\phi = 10^{19}$ s can reach about 386 and 1 at 100 GeV and 65 TeV at IceCube, respectively, as shown in figure 2 (see the red solid line). Figure 2 also presents MCPs with $\epsilon^2 = 10^{-9}$ (see the blue dash line) and $\epsilon^2 = 10^{-10}$ (see the green dot line) could be detected below about 5 TeV and 380 GeV at IceCube, respectively, when $\tau_\phi = 10^{19}$ s.

6 Discussion and conclusion

Ref. [46] presents an analysis of neutrino signals due to the DM annihilation in the Sun with 6 years of IceCube data. This analysis has not found any significant indication of neutrinos due to the DM annihilation in the Sun. Since the MCP and neutrino signals are hard to distinguish at IceCube, it is a reasonable assumption that no events are observed in the measurement of MCPs due to the decay of ϕ in the Sun at IceCube in 6 years. The corresponding upper limit on MCP flux at 90% C.L. was calculated with the Feldman-Cousins approach [47] (see the black solid line in figure 3). Figure 3 also presents the fluxes of expected MCPs with $\epsilon^2 = 10^{-8}$ (red solid line), 10^{-9} (blue dash line) and 10^{-10} (green dot line). That limit excludes the MCP fluxes with $\epsilon^2 = 10^{-8}$, 10^{-9} and 10^{-10} below about 25 TeV, 1.8 TeV and 200 GeV, respectively.

With $\epsilon^2 = 10^{-8}$, 10^{-9} and 10^{-10}, hence, the MCPs from the Sun can be measured in the energy ranges 25–65 TeV, 1.8–5 TeV and 200–380 GeV at IceCube, respectively, when $\tau_\phi = 10^{19}$ s. Based on the results described above, it is a reasonable conclusion that those MCPs could be directly detected in the energy range O(100GeV)-O(10TeV) at IceCube when $\epsilon^2 \gtrsim 10^{-10}$. Since these constraints are only given by the assumptions mentioned above, certainly, the experimental collaborations, like the IceCube collaboration, should be encouraged to conduct an unbiased analysis with the data of IceCube.

Since Φ_{MCP} is proportional to $\dfrac{1}{\tau_\phi}$ (see eq. (2.3)), the above results actually depends on the lifetime of heavy DM, τ_ϕ. If τ_ϕ varies from 10^{20} s to 10^{21} s, the numbers of expected MCPs with IceCube are less by from 1 to 2 orders of magnitude than that with $\tau_\phi = 10^{19}$ s, respectively.

Likewise, the upper limit for ϵ^2 at 90% C.L. can be calculated with the Feldman-Cousins approach. Figure 4 shows these limits with $\tau_\phi = 10^{19}$ s (see red solid line), 10^{20} s (see blue dash line) and 10^{21} s (see green dot line), respectively. If the heavy DM mass, m_ϕ, is equal to $3\,\mathrm{TeV}$ (the corresponding MCP energy is just $1.5\,\mathrm{TeV}$), as shown in figure 4, the region of $\epsilon^2 > 3.5 \times 10^{-11}$ (that is $\epsilon > 5.9 \times 10^{-6}$) is ruled out when $\tau_\phi = 10^{19}$ s.

The MCP mass, m_{MCP}, is at least taken to be less than $10\,\mathrm{MeV}$, since it is assumed that the MCP mass are much less than that of a proton, as mentioned in section 1. So the region of $\epsilon > 5.9 \times 10^{-6}$ is ruled out at 90% C.L. in the m_{MCP}-ϵ plane, when $m_{MCP} < 10\,\mathrm{MeV}$. This result is shown in figure 5. To compare to other observations on MCPs, this figure also shows the ϵ bounds from cosmological and astrophysical observations [22, 23, 48, 49], accelerator and fixed-target experiments [24, 25], experiments for decay of ortho-positronium [28] and Lamb shift [29]. A new region of $0.6\,\mathrm{MeV} < m_{MCP} < 10\,\mathrm{MeV}$ and $6 \times 10^{-6} < \epsilon \lesssim 10^{-4}$ is ruled out in the m_{MCP}-ϵ plane with 6 year of IceCube data, as shown in figure 5.

The MCPs from the Sun's core could be more easily detected with IceCube, compared to those from the Earth's core (although it is closer to the IceCube detector than the Sun), since the ϕ accumulation in the Sun is much greater than that in the Earth [34]. The numbers of expected MCPs in the case of the Earth are less by about 2 orders of magnitude than those in the case of the Sun, as I roughly evaluated them. The region of $\epsilon \gtrsim 10^{-3}$ is ruled out in the case of the Earth when $\tau_\phi = 10^{19}$ s. Meanwhile, the numbers of expected MCPs from the decay of the galactic and extra-galactic ϕ's were roughly evaluated at IceCube. They are less by about 2 times than that in the case of the Sun. The ϵ below limit in the galactic and extra-galactic case is about 10^{-5} when $\tau_\phi = 10^{19}$ s.

Since the decay of ϕ's into MCPs can lead to extra energy injection during recombination and reionization eras in the early universe, the parameters in this DM scenario may be constrained by early universe observations. Since the ϕ lifetime is much greater than the age of the Universe, however, $\Omega_{MCPs}h^2 \lesssim 10^{-12}\Omega_{DM}h^2$ in this scenario. Ref. [50] presented that the cosmological abundance of MCPs was strongly constrained by the Planck data, that was $\Omega_{MCPs}h^2 < 0.001$. I also arrived at the upper limit of $\epsilon \gtrsim 10^{-6}$ with the Planck data when $m_{MCP} = 1\,\mathrm{MeV}$, according to ref. [50]. This is in consistence with my result mentioned above. Thus, the parameters in this DM scenario can't be constrained by the present early universe observations.
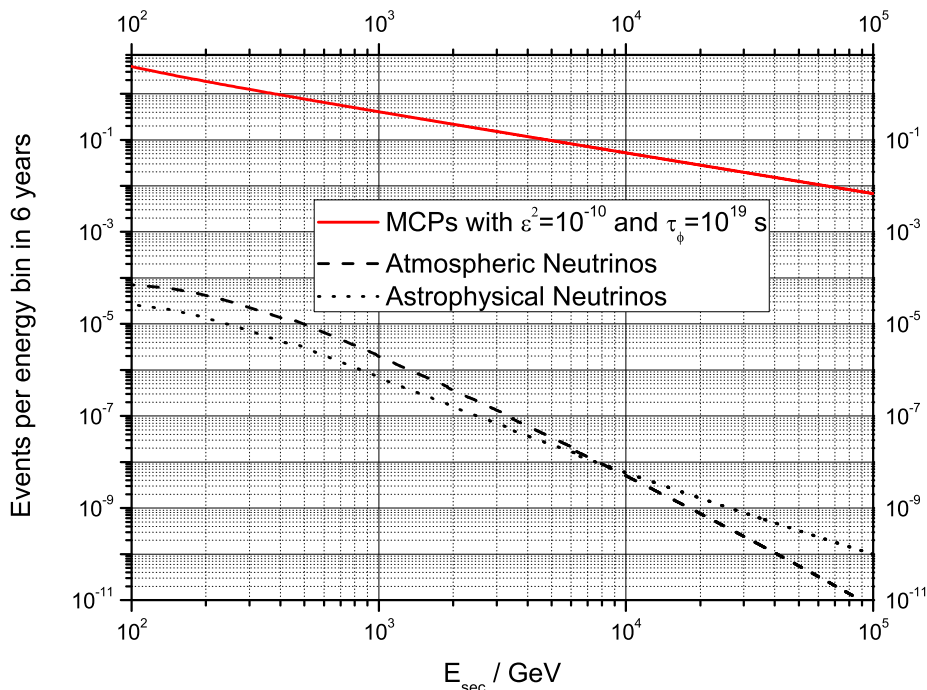
Acknowledgments

Figure 1. Distributions of expected MCPs with $\tau_\phi = 10^{19}$ s and $\epsilon^2 = 10^{-10}$ and astrophysical and atmospheric neutrinos. Their energy bins are $100\,\text{GeV}$.
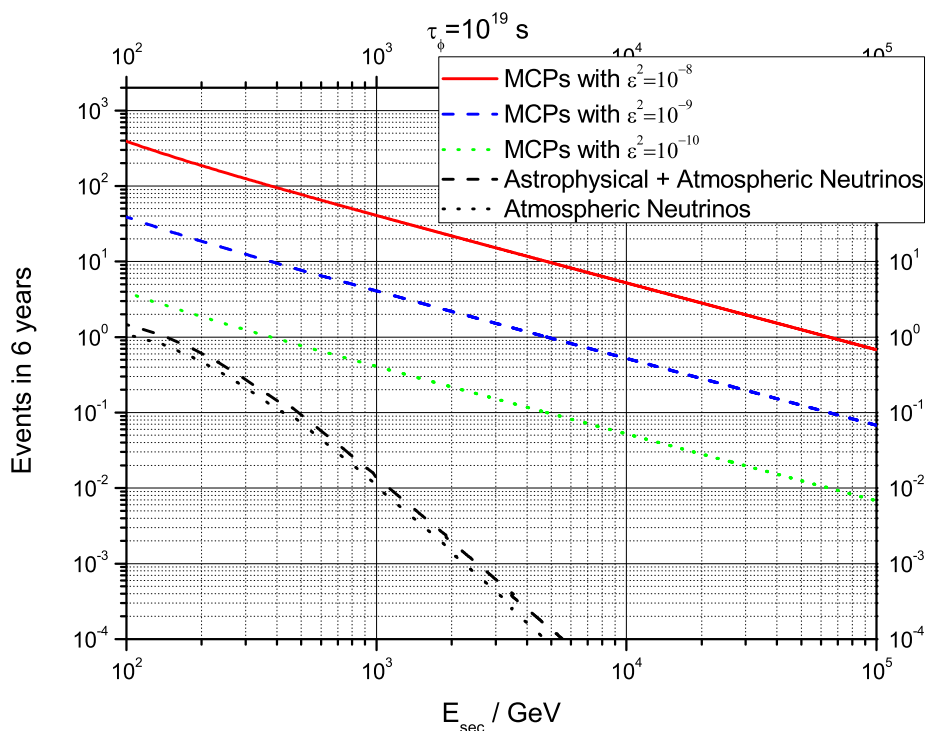

Figure 2. With the different ϵ^2 ($= 10^{-10}$, 10^{-9} and 10^{-8}), the numbers of expected MCPs were evaluated assuming 6 years of IceCube data, respectively. The evaluation of numbers of expected neutrinos was performed by integrating over the regions caused by one standard energy and median angular uncertainties.
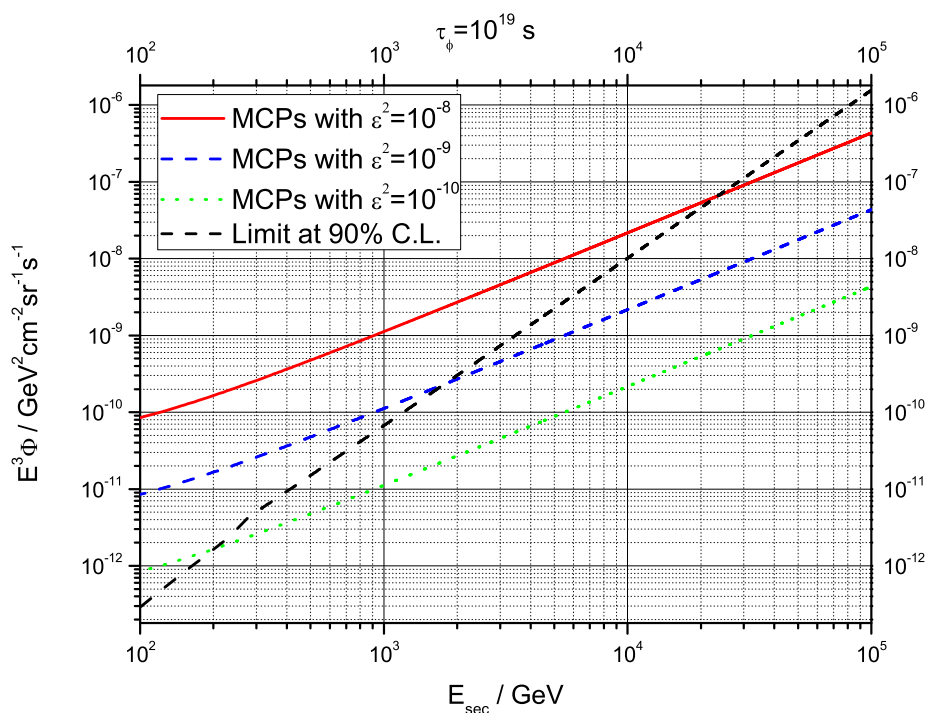
Figure 3. With the different ϵ^2 (= 10^{-10}, 10^{-9} and 10^{-8}), the fluxes of expected MCPs were estimated at IceCube, respectively. Assuming no observation at IceCube in 6 years, the upper limit at 90% C.L. was also computed.
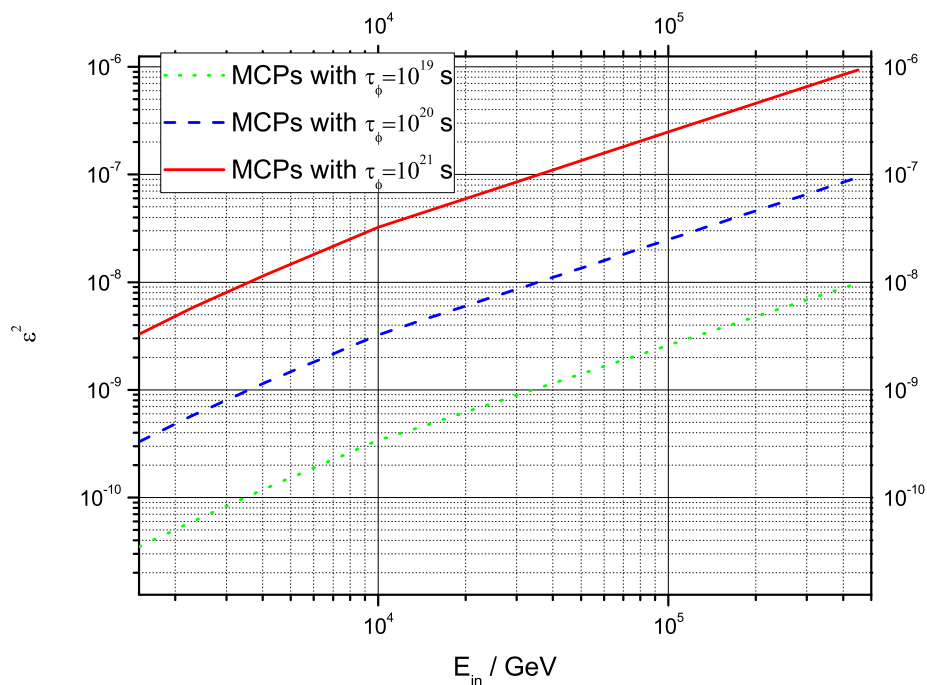
Figure 4. With the different τ_ϕ (= 10^{19} s, 10^{20} s and 10^{21} s), the upper limit on ϵ^2 at 90% C.L. was computed, respectively, assuming no observation at IceCube in 6 years.
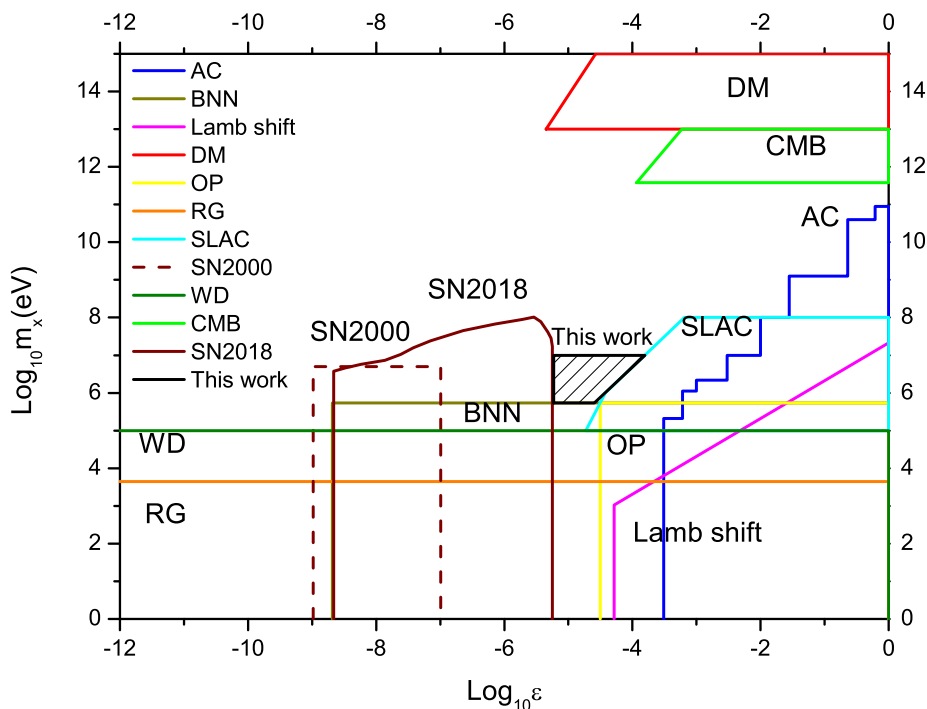
Figure 5. If $m_\phi = 3\,\text{TeV}$, with $\tau_\phi = 10^{19}$ s, a new region (shaded region) is ruled out in the m_{MCP} vs. ϵ plane, when $m_{MCP} < 10\,MeV$ and $\epsilon > 5.9 \times 10^{-6}$ (this work). Meanwhile, the bounds from plasmon decay in red giants (RG) [23], plasmon decay in white dwarfs (WD) [23], cooling of the Supernova 1987A (SN2000 [23], SN2018 [22]), accelerator (AC) [24] and fixed-target experiments (SLAC) [25], the Tokyo search for the invisible decay of ortho-positronium (OP) [28], the Lamb shift [29], big bang nucleosynthesis (BBN) [23], cosmic microwave background (CMB) [48] and dark matter searches (DM) [49] are also plotted on this figure.

References

[1] L. Bergström, *Nonbaryonic dark matter: Observational evidence and detection methods*, *Rept. Prog. Phys.* **63** (2000) 793 [`hep-ph/0002126`] [iNSPIRE].

[2] G. Bertone, D. Hooper and J. Silk, *Particle dark matter: Evidence, candidates and constraints*, *Phys. Rept.* **405** (2005) 279 [`hep-ph/0404175`] [iNSPIRE].

[3] PLANCK collaboration, *Planck 2015 results. XIII. Cosmological parameters*, *Astron. Astrophys.* **594** (2016) A13 [`arXiv:1502.01589`] [iNSPIRE].

[4] XENON collaboration, *First Dark Matter Search Results from the XENON1T Experiment*, *Phys. Rev. Lett.* **119** (2017) 181301 [`arXiv:1705.06655`] [iNSPIRE].

[5] PandaX-II collaboration, *Dark Matter Results From 54-Ton-Day Exposure of PandaX-II Experiment*, *Phys. Rev. Lett.* **119** (2017) 181302 [`arXiv:1708.06917`] [iNSPIRE].

[6] Fermi-LAT collaboration, *Limits on Dark Matter Annihilation Signals from the Fermi LAT 4-year Measurement of the Isotropic Gamma-Ray Background*, *JCAP* **09** (2015) 008 [`arXiv:1501.05464`] [iNSPIRE].

[7] ANTARES and IceCube collaborations, *Combined search for neutrinos from dark matter self-annihilation in the Galactic Center with ANTARES and IceCube*, *Phys. Rev. D* **102** (2020) 082002 [`arXiv:2003.06614`] [iNSPIRE].

[8] ANTARES collaboration, *Limits on Dark Matter Annihilation in the Sun using the ANTARES Neutrino Telescope*, *Phys. Lett. B* **759** (2016) 69 [`arXiv:1603.02228`] [iNSPIRE].

[9] IceCube collaboration, *Search for annihilating dark matter in the Sun with 3 years of IceCube data*, *Eur. Phys. J. C* **77** (2017) 146 [*Erratum ibid.* **79** (2019) 214] [`arXiv:1612.05949`] [iNSPIRE].

[10] CAST collaboration, *New CAST limit on the axion-photon interaction*, *Nature Phys.* 13 (2017) 584.

[11] GlueX collaboration, *Search for photoproduction of axionlike particles at GlueX*, *Phys. Rev. D* **105** (2022) 052007 [`arXiv:2109.13439`] [iNSPIRE].

[12] C.S. Reynolds, M.C.D. Marsh, H.R. Russell, A.C. Fabian, R. Smith, F. Tombesi et al., *Astrophysical limits on very light axion-like particles from Chandra grating spectroscopy of NGC 1275*, *Astrophys. J.* **890** (2020) 59 [`arXiv:1907.05475`] [iNSPIRE].

[13] Double CHOOZ collaboration, *Search for signatures of sterile neutrinos with Double CHOOZ*, *Eur. Phys. J. C* **81** (2021) 775 [`arXiv:2009.05515`] [iNSPIRE].

[14] MINOS+ and Daya Bay collaborations, *Improved Constraints on Sterile Neutrino Mixing from Disappearance Searches in the MINOS, MINOS+, Daya Bay, and Bugey-3 Experiments*, *Phys. Rev. Lett.* **125** (2020) 071801 [`arXiv:2002.00301`] [iNSPIRE].

[15] H. Goldberg and L.J. Hall, *A New Candidate for Dark Matter*, *Phys. Lett. B* **174** (1986) 151 [iNSPIRE].

[16] K. Cheung and T.-C. Yuan, *Hidden fermion as milli-charged dark matter in Stueckelberg Z′ model*, *JHEP* **03** (2007) 120 [`hep-ph/0701107`] [ɪɴSPIRE].

[17] D. Feldman, Z. Liu and P. Nath, *The Stueckelberg Z′ Extension with Kinetic Mixing and Milli-Charged Dark Matter From the Hidden Sector*, *Phys. Rev. D* **75** (2007) 115001 [`hep-ph/0702123`] [ɪɴSPIRE].

[18] B. Holdom, *Two* U(1)*'s and Epsilon Charge Shifts*, *Phys. Lett. B* **166** (1986) 196 [ɪɴSPIRE].

[19] B. Batell and T. Gherghetta, *Localized* U(1) *gauge fields, millicharged particles, and holography*, *Phys. Rev. D* **73** (2006) 045016 [`hep-ph/0512356`] [ɪɴSPIRE].

[20] F. Brummer and J. Jaeckel, *Minicharges and Magnetic Monopoles*, *Phys. Lett. B* **675** (2009) 360 [`arXiv:0902.3615`] [ɪɴSPIRE].

[21] F. Brummer, J. Jaeckel and V.V. Khoze, *Magnetic Mixing: Electric Minicharges from Magnetic Monopoles*, *JHEP* **06** (2009) 037 [`arXiv:0905.0633`] [ɪɴSPIRE].

[22] J.H. Chang, R. Essig and S.D. McDermott, *Supernova 1987A Constraints on sub-GeV Dark Sectors, Millicharged Particles, the QCD Axion, and an Axion-like Particle*, *JHEP* **09** (2018) 051 [`arXiv:1803.00993`] [ɪɴSPIRE].

[23] S. Davidson, S. Hannestad and G. Raffelt, *Updated bounds on millicharged particles*, *JHEP* **05** (2000) 003 [`hep-ph/0001179`] [ɪɴSPIRE].

[24] S. Davidson, B. Campbell and D.C. Bailey, *Limits on particles of small electric charge*, *Phys. Rev. D* **43** (1991) 2314 [ɪɴSPIRE].

[25] A.A. Prinz et al., *Search for millicharged particles at SLAC*, *Phys. Rev. Lett.* **81** (1998) 1175 [`hep-ex/9804008`] [ɪɴSPIRE].

[26] R. Essig, T. Volansky and T.-T. Yu, *New Constraints and Prospects for sub-GeV Dark Matter Scattering off Electrons in Xenon*, *Phys. Rev. D* **96** (2017) 043017 [`arXiv:1703.00910`] [ɪɴSPIRE].

[27] H. Liu and T.R. Slatyer, *Implications of a* 21*-cm signal for dark matter annihilation and decay*, *Phys. Rev. D* **98** (2018) 023501 [`arXiv:1803.09739`] [ɪɴSPIRE].

[28] T. Mitsui, R. Fujimoto, Y. Ishisaki, Y. Ueda, Y. Yamazaki, S. Asai et al., *Search for invisible decay of orthopositronium*, *Phys. Rev. Lett.* **70** (1993) 2265 [ɪɴSPIRE].

[29] S.R. Lundeen and F.M. Pipkin, *Measurement of the Lamb Shift in Hydrogen, N = 2*, *Phys. Rev. Lett.* **46** (1981) 232 [ɪɴSPIRE].

[30] Y. Farzan and M. Rajaee, *Dark matter decaying into millicharged particles as a solution to AMS-02 positron excess*, *JCAP* **04** (2019) 040 [`arXiv:1901.11273`] [ɪɴSPIRE].

[31] R. Aloisio, S. Matarrese and A.V. Olinto, *Super Heavy Dark Matter in light of BICEP2, Planck and Ultra High Energy Cosmic Rays Observations*, *JCAP* **08** (2015) 024 [`arXiv:1504.01319`] [ɪɴSPIRE].

[32] A. Esmaili, A. Ibarra and O.L.G. Peres, *Probing the stability of superheavy dark matter particles with high-energy neutrinos*, *JCAP* **11** (2012) 034 [`arXiv:1205.5281`] [ɪɴSPIRE].

[33] Y. Xu, *Measurement of high energy dark matter from the Sun at IceCube*, *JHEP* **12** (2021) 035 [`arXiv:2106.02202`] [ɪɴSPIRE].

[34] P. Baratella, M. Cirelli, A. Hektor, J. Pata, M. P IIBeleht and A. Strumia, *PPPC 4 DMν: a Poor Particle Physicist Cookbook for Neutrinos from Dark Matter annihilations in the Sun*, *JCAP* **03** (2014) 053 [`arXiv:1312.6408`] [ɪɴSPIRE].

[35] G. Jungman, M. Kamionkowski and K. Griest, *Supersymmetric dark matter*, *Phys. Rept.* **267** (1996) 195 [`hep-ph/9506380`] [ɪɴSPIRE].

[36] R.F. Stein and A. Nordlund, *Simulations of Solar Granulation. I. General Properties*, *Astrophys. J.* 499 (1998) 914.

[37] M. Klein and T. Riemann, *Electroweak interactions probing the nucleon structure*, *Z. Phys. C* **24** (1984) 151 [ɪɴSPIRE].

[38] S. Alekhin, J. Blümlein, S. Moch and R. Placakyte, *Parton distribution functions, α_s, and heavy-quark masses for LHC Run II*, *Phys. Rev. D* **96** (2017) 014011 [`arXiv:1701.05838`] [ɪɴSPIRE].

[39] M.M. Block, P. Ha and D.W. McKay, *Ultrahigh energy neutrino scattering: An Update*, *Phys. Rev. D* **82** (2010) 077302 [`arXiv:1008.4555`] [ɪɴSPIRE].

[40] IceCube collaboration, *Sensitivity of the IceCube detector to astrophysical sources of high energy muon neutrinos*, *Astropart. Phys.* **20** (2004) 507 [`astro-ph/0305196`] [ɪɴSPIRE].

[41] IceCube collaboration, *Searches for Extended and Point-like Neutrino Sources with Four Years of IceCube Data*, *Astrophys. J.* **796** (2014) 109 [`arXiv:1406.6757`] [ɪɴSPIRE].

[42] IceCube collaboration, *The IceCube high-energy starting event sample: Description and flux characterization with 7.5 years of data*, *Phys. Rev. D* **104** (2021) 022002 [`arXiv:2011.03545`] [ɪɴSPIRE].

[43] T.S. Sinegovskaya, A.D. Morozova and S.I. Sinegovsky, *High-energy neutrino fluxes and flavor ratio in the Earth's atmosphere*, *Phys. Rev. D* **91** (2015) 063011 [`arXiv:1407.3591`] [ɪɴSPIRE].

[44] IceCube collaboration, *Combining Maximum-Likelihood with Deep Learning for Event Reconstruction in IceCube*, PoS-ICRC2021-1065.

[45] IceCube collaboration, *Energy Reconstruction Methods in the IceCube Neutrino Telescope*, 2014 *JINST* **9** P03009 [`arXiv:1311.4767`] [ɪɴSPIRE].

[46] IceCube collaboration, *Search for secluded dark matter with 6 years of IceCube data*, in *37th International Cosmic Ray Conference*, (2021) [`arXiv:2107.10778`] [ɪɴSPIRE].

[47] G.J. Feldman and R.D. Cousins, *A Unified approach to the classical statistical analysis of small signals*, *Phys. Rev. D* **57** (1998) 3873 [`physics/9711021`] [ɪɴSPIRE].

[48] S.L. Dubovsky, D.S. Gorbunov and G.I. Rubtsov, *Narrowing the window for millicharged particles by CMB anisotropy*, *JETP Lett.* **79** (2004) 1 [`hep-ph/0311189`] [ɪɴSPIRE].

[49] J. Jaeckel and A. Ringwald, *The Low-Energy Frontier of Particle Physics*, *Ann. Rev. Nucl. Part. Sci.* **60** (2010) 405 [`arXiv:1002.0329`] [ɪɴSPIRE].

[50] A.D. Dolgov, S.L. Dubovsky, G.I. Rubtsov and I.I. Tkachev, *Constraints on millicharged particles from Planck data*, *Phys. Rev. D* **88** (2013) 117701 [`arXiv:1310.2376`] [ɪɴSPIRE].